

# Line shape of the $\mu\text{H}(3p - 1s)$ hyperfine transitions

D. S. Covita,<sup>1,2</sup> D. F. Anagnostopoulos,<sup>3</sup> H. Gorke,<sup>4</sup> D. Gotta,<sup>5</sup> A. Gruber,<sup>6</sup> A. Hirtl,<sup>6</sup>  
T. Ishiwatari,<sup>6</sup> P. Indelicato,<sup>7</sup> E.-O. Le Bigot,<sup>7</sup> M. Nekipelov,<sup>5</sup> J. M. F. dos Santos,<sup>1</sup>  
Ph. Schmid,<sup>6</sup> L. M. Simons,<sup>2,\*</sup> M. Trassinelli,<sup>7,†</sup> J. F. C. A. Veloso,<sup>8</sup> and J. Zmeskal<sup>6</sup>

<sup>1</sup>*Dept. of Physics, Coimbra University, P-3000 Coimbra, Portugal*

<sup>2</sup>*Paul Scherrer Institut (PSI), CH 5232-Villigen, Switzerland*

<sup>3</sup>*Dept. of Materials Science and Engineering, University of Ioannina, Ioannina, GR-45110, Greece*

<sup>4</sup>*Zentralabteilung für Elektronik, Forschungszentrum Jülich GmbH, D-52425 Jülich, Germany*

<sup>5</sup>*Institut für Kernphysik, Forschungszentrum Jülich GmbH, D-52425 Jülich, Germany*

<sup>6</sup>*Stefan Meyer Institut for Subatomic Physics, Austrian Academy of Sciences, A-1090 Vienna, Austria*

<sup>7</sup>*Laboratoire Kastler Brossel, UPMC-Paris 6, ENS,*

*CNRS; Case 74, 4 place Jussieu, F-75005 Paris, France*

<sup>8</sup>*Dept. of Physics, Aveiro University, P-3810 Aveiro, Portugal*

(Dated: November 7, 2018)

The  $(3p - 1s)$  X-ray transition to the muonic hydrogen ground state was measured with a high-resolution crystal spectrometer. A Doppler effect broadening of the X-ray line was established which could be attributed to different Coulomb de-excitation steps preceding the measured transition. The assumption of a statistical population of the hyperfine levels of the muonic hydrogen ground state was directly confirmed by the experiment and measured values for the hyperfine splitting can be reported. The results allow a decisive test of advanced cascade model calculations and establish a method to extract fundamental strong-interaction parameters from pionic hydrogen experiments.

PACS numbers: 36.10.-k

A series of experiments has been conducted at the Paul Scherrer Institut (PSI), Switzerland, to extract the isospin separated pion-nucleon scattering lengths from the observation of X-ray transitions feeding the ground state of pionic hydrogen [1, 2, 3]. With X-ray energies of about 2-3 keV and values for the strong-interaction shift and broadening being of about 7 eV and 1 eV, respectively, the use of a high resolution Bragg spectrometer was mandatory to reach the envisaged precision on the per cent level.

The experimental difficulties are considerable, especially for the isovector scattering length, which is equivalent to the determination of the strong interaction broadening. It requires to extract from the measured line shape a Lorentzian profile representing the natural width, which is convoluted with the spectrometer response and several contributions owing to the Doppler broadenings from different high velocity states of the exotic atom.

High velocity states develop in exotic hydrogen atoms during the atomic de-excitation cascade. As the system is electrically neutral, it may dive deeply into the electron cloud of a neighbouring hydrogen molecule. Such close collisions strongly influence the atomic cascade. The most important of these processes are the so-called Coulomb transitions [4, 5, 6], collision-induced radiationless de-excitations, where the released energy is shared between the exotic atom and a normal hydrogen atom as recoil partner. During the cascade, acceleration due to Coulomb transitions and deceleration by elastic and inelastic collisions compete, which results in a complex and level dependent kinetic energy distribution.

Historically, the first evidence for high velocity states

was found in the charge exchange reaction  $\pi^-p \rightarrow \pi^0n$  with stopped pions as Doppler broadening of the time-of-flight (TOF) of the monoenergetic neutrons [7]. Later on detailed studies confirmed that Coulomb de-excitation substantially affects the kinetic energy of  $\pi\text{H}$  [8] and  $\mu\text{H}$  atoms [9] even at lowest densities. From the TOF spectra, several components were identified and attributed to specific Coulomb transitions. Hints for the influence of the Doppler broadening in X-ray transitions were identified in experiments measuring the strong-interaction width of the  $\pi\text{H}$  ground state [2, 3]. A correction for the cascade-induced broadening is therefore indispensable for a proper extraction of the hadronic contribution to the X-ray line width. However, the high precision information from the reaction  $\pi^-p \rightarrow \pi^0n$  cannot be directly transferred to X-ray studies. Charge exchange occurs from  $ns$  states, mainly with principal quantum numbers  $n = 3 - 5$  of the  $\pi^-p$  system, whereas the initial states for K X-ray emission are  $np$  levels. Consequently, the preceding cascade steps for the two processes are different and the Doppler contributions to the X-ray line shape deviate from the ones derived from neutron TOF experiments.

As the intensities of the X-ray transitions strongly depend on the hydrogen density, there was a first approach to extract information about the cross sections of Coulomb de-excitation from intensity studies. Different processes like Stark transitions and external Auger effect, however, are overwhelming in their importance for the X-ray intensity compared to Coulomb de-excitation. In consequence, the kinetic energy  $T_{kin}$  of the exotic hydrogen atom was used in earlier cascade codes (the so-called Standard Cascade Model: SCM) as a fitting pa-

parameter with values around  $T_{kin} = 1$  eV, which explained the measured intensities with sufficient accuracy [10].

Based on the SCM an extended standard cascade model (ESCM) was developed. It is a new approach to calculate the Doppler contributions to neutron TOF and exotic hydrogen X-ray spectra by taking into account the competing processes in each de-excitation step and a kinetic energy distribution at the time of X-ray emission is provided [11]. An example of such a kinetic energy distribution for muonic hydrogen in the  $3p$  state is shown in Fig. 1. Monoenergetic lines corresponding to specific Coulomb transitions  $n \rightarrow n'$  are smeared out because of the numerous elastic collisions after the Coulomb transition and before X-ray emission. The validity of ESCM calculations cannot be tested directly in pionic hydrogen as the strong-interaction broadening completely masks the fine details of the various Doppler contributions.

Muonic hydrogen as a purely electromagnetic twin system to pionic hydrogen offers itself as an ideal candidate for the direct observation of the Coulomb de-excitation. Ideally, it could be used as a test of the validity of the ESCM by reproducing the line shape of muonic hydrogen X-ray transitions in a fitting routine with the predictions of the ESCM as input. The theoretical values for the ground state hyperfine splitting, and more important, for the relative intensity of the transitions feeding the triplet and singlet components should be obtained. The ground-state hyperfine splitting is calculated to be  $182.725 \pm 0.062$  meV [12]. A relative statistical population of 3:1 is expected for the triplet and singlet components.

An understanding of the atomic cascade in exotic hydrogen is needed in other experimental studies as well, e.g., (i) for the precision determination of the proton charge radius from the muonic hydrogen  $2s-2p$  Lamb shift [9, 13] or (ii) in the measurement of the induced pseudoscalar coupling in muon capture by the proton [14, 15, 16].

The experiment was performed at the  $\pi E5$  channel of the proton accelerator at PSI, which provides a low-energy pion beam with intensities of up to a few  $10^8$ /s. Pions of  $112$  MeV/c were injected into the cyclotron trap II [1] and decelerated using a set of degraders optimized to the number of muon stops by measuring X-rays from muonic helium. Muonic atoms are formed by slow muons originating from the decay of almost stopped pions close to or in a cylindrical cryogenic target cell of 22 cm length and 5 cm in diameter in the center of the trap. The cell was filled with hydrogen gas cooled down to 25K at 1 bar absolute pressure, which corresponds to a density equivalent to 12.5 bar at room temperature. X-radiation could exit the target cell axially through a  $5 \mu\text{m}$  thick mylar<sup>®</sup> window.

X-rays from the  $\mu\text{H}(3p-1s)$  transition were measured with a Johann-type Bragg spectrometer equipped with a spherically bent Si(111) crystal having a radius of curvature of  $2982.2 \pm 0.3$  mm and a free diameter of 90 mm [18].

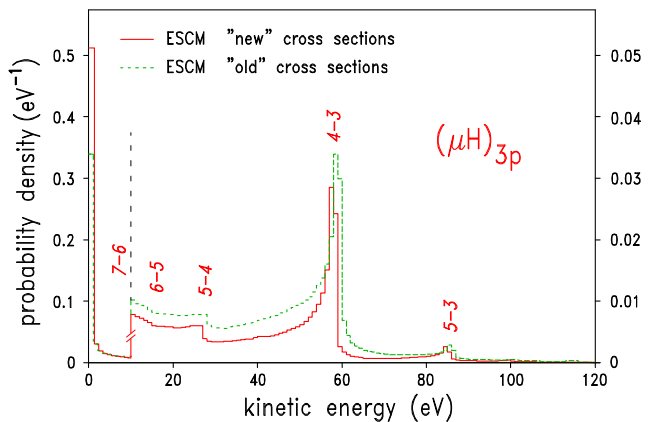


FIG. 1: Kinetic energy distribution of  $\mu\text{H}$  atoms in the  $3p$  state for a hydrogen density equivalent to 12.5 bar as predicted from the ESCM [11] using a) cross sections calculated by [11] (dashed curve) and b) recalculated cross sections [17] stimulated by the present experiment (solid curve). Numbers indicate the corresponding Coulomb transitions  $n \rightarrow n'$ . Note the change of the vertical scale at 10 eV.

Such a spectrometer is able to measure simultaneously an energy interval according to the width of the X-ray source when using a correspondingly extended X-ray detector, in this case a  $3 \times 2$  array of charge-coupled devices (CCDs) covering in total 72 mm in height and 48 mm in width [19]. A pixel size of  $40 \mu\text{m}$  provides the two dimensional position resolution necessary in order to measure the diffraction image. The background rejection capability of CCDs together with a massive concrete shielding suppresses efficiently events from beam induced reactions. In total almost 10000 events were collected for the  $\mu\text{H}(3p-1s)$  line (Fig. 2).

The spin-averaged  $\mu\text{H}(3p-1s)$  transition energy is calculated to be  $2249.461 \pm 0.001$  eV with a radiative line width of  $0.3 \mu\text{eV}$  [20]. The  $3p$ -level splittings amount to a few meV only [21]. Hence, two components with identical response functions are sufficient to describe the  $(3p-1s)$  line. The spectrometer response was determined using narrow X-rays from helium-like argon as outlined in [22, 23]. Applying this method to chlorine and sulfur, an extrapolation yields a resolution of  $272 \pm 3$  meV (FWHM) at the  $\mu\text{H}(3p-1s)$  transition energy, which is significantly narrower than the observed line width (Fig. 2). Details may be found elsewhere [24].

As a first trial to include the Doppler broadening caused by Coulomb de-excitation the kinetic energy distribution given by the ESCM result of [11] (Fig. 1) was taken directly as an input for the fitting of the line shape, which was done by means of the MINUIT package [25]. A comparison to the measured line shape yields a poor reduced  $\chi^2$  of  $\chi_r^2 = 1.353$  only (Fig. 2-dashed dotted line).

It is evident that this ESCM prediction with a weight of 36% only for the low-energy component  $T_{kin} \leq 2$  eV underestimates substantially the fraction of X-rays with

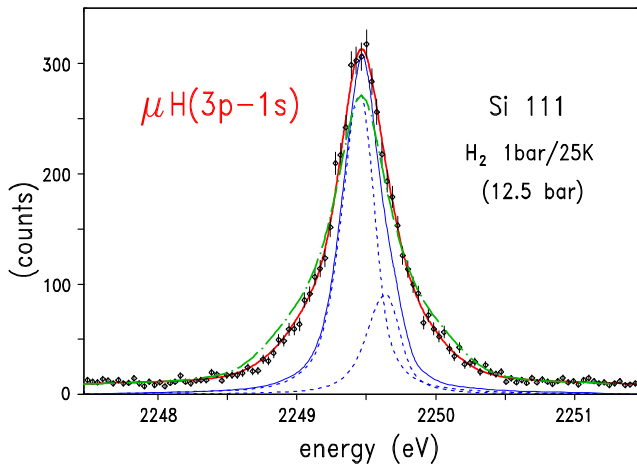


FIG. 2: Line shape of the  $\mu\text{H}(3p-1s)$  transition as measured with a Si (111) crystal in first order. One energy bin corresponds to 2 CCD pixels or 37.2 meV. The spectrometer response (thin solid line) represents the expected line shape formed by the two hyperfine components (dashed lines) without any Doppler broadening (normalised to the peak height after background subtraction). Including Coulomb de-excitation by using long standing cross sections [11] yields a poor description (dashed-dotted) of the line shape. The “best fit” in a “model free” approach (see text) is shown by thick solid line following the data. A very good fit – being indistinguishable by eye from the “model free” approach – was found when using for the ESCM calculation the recently recalculated cross sections [17].

small Doppler shifts. This reveals that cross sections responsible for the development of such low energies coming from an interplay of Coulomb de-excitation and elastic collisions could still be deficient. In addition, the cascade calculation starting at  $n = 8$  possibly neglects stronger effects from Coulomb de-excitation in the outer shells ( $n > 11$ ), where the ESCM uses a classical trajectory Monte-Carlo approach.

Consequently, as a further approach a “model free” method was applied, which has already been used in the case of the neutron TOF spectra [8]. The Doppler contributions from Coulomb de-excitation to the  $\mu\text{H}(3p-1s)$  line shape were determined by modelling the kinetic energy distribution with several rectangular boxes, the number of which is assessed by the transitions in the preceding cascade.

Several sets of kinetic energy boxes were investigated including besides  $\Delta n = 1$  also  $\Delta n = 2$  Coulomb transitions. Hyperfine splitting, i.e., both line positions, relative population, (flat) background, and the relative weight of the boxes were free parameters in the fit. The sum of the relative weights of the boxes was always normalized to one.

It is a major result of this study, that three narrow boxes are essential but also sufficient to model a kinetic energy distribution yielding a good fit to the

$\mu\text{H}(3p-1s)$  line shape: (i) one low-energy component below  $T_{kin} = 2$  eV collecting  $\mu\text{H}$  atoms which gained their energy from  $n \geq 10$  Coulomb transitions and/or high velocity systems degraded by collisions, and (ii) two at higher energies corresponding to the de-excitation steps  $n = 5 \rightarrow 4$  ( $T_{kin} = 26.9$  eV) and  $n = 4 \rightarrow 3$  ( $T_{kin} = 58.2$  eV).

A  $\chi^2$  analysis shows that a weight of  $\approx 60\%$  is mandatory for the low-energy component. In case of the high-energy components the fit is only sensitive to the relative weight and the central value. Extending the boundaries up to  $\pm 30\%$  of the central values, affects the result by less than 1.4 standard deviations. Therefore, the kinetic energy distribution could be condensed to three narrow intervals.

The best reduced  $\chi^2$  is found to be  $\chi_r^2 = 0.947$  for the kinetic energy intervals set to  $[0-1.8]$ ,  $[26.4-27.4]$ , and  $[57.7-58.7]$  eV resulting in relative weights of  $(61 \pm 2)\%$ ,  $(25 \pm 3)\%$ , and  $(14 \pm 4)\%$  (Fig. 2: “best fit” in the “model free” approach). Uncertainties represent statistical errors only.

A correlation study of hyperfine splitting and relative population was performed by using the three kinetic energy intervals found in the above mentioned analysis, but with their weights, total intensity, and background kept as free parameters. The best  $\chi_r^2 = 0.941$  is obtained for a hyperfine splitting of  $211 \pm 19$  meV, a triplet to singlet population of  $(3.59 \pm 0.51) : 1$  (Fig. 3–A), and relative weight of  $61 \pm 1\%$  for the low-energy component, where errors correspond to  $1\sigma$ . The 1, 1.5, and  $2\sigma$  contours are also shown. When fixing the hyperfine splitting to the theoretical value, the best fit is obtained for a triplet to singlet population of  $(2.90 \pm 0.21) : 1$  (Fig. 3–B), very close to the statistical value. The  $\chi^2$  differs only by 1.5  $\sigma$  from the best value.

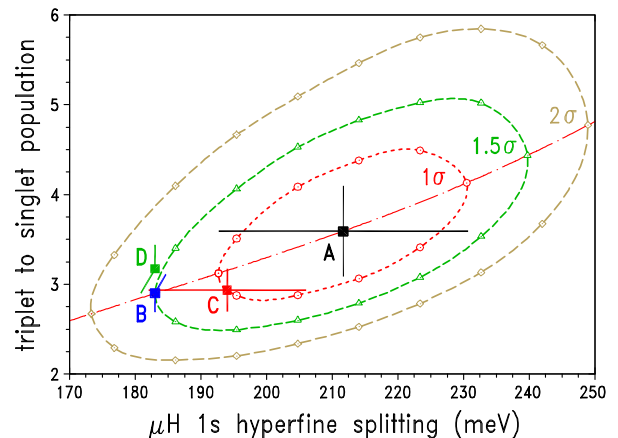


FIG. 3:  $\chi^2$  contour for the correlation of hyperfine splitting and relative population in the “model free” approach. The dashed-dotted line displays the location of the minimum  $\chi^2$  for the corresponding hyperfine splitting. (A – D: see text).

The results from the present experiment led to a reconsideration of cross sections involved in exotic-hydrogen de-excitation. In a fully quantum-mechanical close-coupling approach, elastic scattering, Stark transitions and Coulomb de-excitation now have been calculated in a unified manner [5, 6, 26].

Including these cross-section results in the ESCM model [17], the relative weight of the low energies ( $T_{kin} \leq 2\text{eV}$ ) increases to 55%, which is closer to the constraint found in the “model free” approach. A fit to the measured  $\mu\text{H}(3p-1s)$  line shape by using directly the new kinetic energy distribution (Fig.1) yields a much better description of the data (Fig.2). Leaving hyperfine splitting and triplet to singlet intensity ratio as free parameters, values were obtained of  $194 \pm 12\text{meV}$  for the hyperfine splitting and  $(2.94 \pm 0.24):1$  for the triplet to singlet intensity ratio (Fig. 3-C). The striking agreement is indicated by  $\chi_r^2 = 0.997$ . When fixing the splitting to the theoretical value the relative triplet to singlet population becomes  $(3.17 \pm 0.27):1$  (Fig. 3-D).

Another process, which may affect the line shape, is due to molecule formation with subsequent radiative decay  $(\mu p)_{nl} + H_2 \rightarrow [(\mu pp)^* p ee]^* \rightarrow [(\mu pp) p ee]^* + \gamma$  [27, 28]. If radiative decay contributes significantly, a line broadening or even satellites at the low-energy side are expected. In the case of  $\mu pp$ , a branching ratio for radiative decay was predicted at the few per cent level [29, 30]. However, in this experiment, no evidence was found at the 1% level for any broadening except from Coulomb de-excitation. The result is corroborated from the absence of any density dependence of the  $\pi\text{H}(3p-1s)$  transition energy [3].

To summarize, the line shape of the  $\mu\text{H}(3p-1s)$  transition was measured with a high resolution Bragg spectrometer. The influence of Coulomb de-excitation was directly seen from a line broadening compared to the spectrometer resolution. By using a “model free” approach various Doppler contributions are identified, which are attributed to preceding Coulomb transitions. A large fraction of the  $\mu\text{H}$  systems are found to have kinetic energies below 2 eV. The measurement yields the  $\mu\text{H}$  ground state hyperfine splitting as calculated from QED and confirms experimentally the statistical population of the triplet and singlet  $1s$  states. The measurement triggered a new calculation of cross sections resulting in a significantly improved description of the  $\mu\text{H}(3p-1s)$  line shape and serves as a basis for a further evaluation of the determination of the isovector scattering amplitude from pionic hydrogen data with increased precision.

It is a pleasure to thank V.P.Popov and V.N.Pomerantsev for the possibility to use their recent theoretical development. The continuous theoretical support of V.E.Markushin and T.S.Jensen is gratefully acknowledged. We would like to thank B. Leoni, N. Dolfus, L. Stohwasser, and K.-P. Wieder for

the technical assistance. The Bragg crystal was manufactured by Carl Zeiss AG, Oberkochen, Germany. Partial funding and travel support was granted by FCT (Lisbon) and FEDER (PhD grant SFRH/BD/18979/2004 and project PTDC/FIS/82006/2006) and the Germaine de Staël exchange program. This work is part of the PhD thesis of one of us (D.S.C., Univ. of Coimbra, 2008).

---

\* present address: Dept. of Physics, Coimbra University, P-3000 Coimbra, Portugal

† present address: Inst. des NanoSciences de Paris, CNRS UMR7588 and UMPC-Paris 6, F-75015 Paris, France

- [1] PSI proposal R-98-01, [www.fz-juelich.de/ikp/exotic-atoms](http://www.fz-juelich.de/ikp/exotic-atoms).
- [2] H.-Ch. Schröder et al., Eur. Phys. J C **21**, 473 (2001).
- [3] D. Gotta et al., Lect. Notes Phys. **745**, 165 (2008).
- [4] L. Bracci and G. Fiorentini, Nuovo Cim. A, **43**, 9 (1978).
- [5] G. Ya. Korenman, V. N. Pomerantsev, and V. P. Popov, JETP. Lett. **81**, 543 (2005).
- [6] V. N. Pomerantsev and V. P. Popov, JETP. Lett. **83**, 331 (2006); Phys. Rev. A **73**, 040501(R) (2006).
- [7] J. B. Czirr et al., Phys. Rev. **130**, 341 (1963).
- [8] A. Badertscher et al., Europhys. Lett. **54**, 313 (2001), and references therein.
- [9] R. Pohl et al., Phys. Rev. Lett. **97**, 193402 (2006).
- [10] E. Borie and M. Leon, Phys. Rev. A **21**, 1460 (1980).
- [11] T. S. Jensen and V. E. Markushin, Eur. Phys. J. D **19**, 165 (2002); Eur. Phys. J. D **21**, 261 (2002); Eur. Phys. J. D **21**, 271 (2002).
- [12] A. P. Martynenko and R. N. Faustov, JETP **98**, 39 (2004).
- [13] R. Pohl et al., Can. J. Phys. **83**, 339 (2005).
- [14] D. F. Measday, Phys. Rep. **354**, 243 (2001).
- [15] T. Gorringer and H. W. Fearing, Rev. Mod. Phys. **76**, 31 (2004).
- [16] V. A. Andreev et al., Phys. Rev. Lett. **99**, 032002 (2007).
- [17] T. S. Jensen, V. N. Pomerantsev, and V. P. Popov, arXiv:0712.3010v1 [nucl-th] (2007).
- [18] D. Gotta, Prog. Part. Nucl. Phys. **52**, 133 (2004).
- [19] N. Nelms et al., Nucl. Instr. Meth. A **484**, 419 (2002).
- [20] P. Indelicato, unpublished (2008).
- [21] K. Pachucki, Phys. Rev. A **53**, 2092 (1996).
- [22] D. F. Anagnostopoulos et al., Nucl. Instr. Meth. A **545**, 217 (2005).
- [23] M. Trassinelli et al., J. Phys., Conf. Ser. **58**, 129 (2007).
- [24] D. S. Covita, thesis, Univ. of Coimbra (2008), unpublished.
- [25] F. James and M. Roos, Comput. Phys. Commun. **10**, 343 (1975).
- [26] V. P. Popov and V. N. Pomerantsev, arXiv:0712.3111v1 [nucl-th] (2007).
- [27] D. Taqqu, AIP Conf. Proc. **181**, 217 (1989).
- [28] S. Jonsell, J. Wallenius, P. Froelich, Phys. Rev. A **59**, 3440 (1999).
- [29] E. Lindroth, J. Wallenius, S. Jonsell, Phys. Rev. A **68**, 032502 (2003); Phys. Rev. A **69**, 059903(E) (2004).
- [30] S. Kilic, J.-P. Karr, L. Hilico, Phys. Rev. A **70**, 042506 (2004).